Asian Journal of Chemistry; Vol. 36, No. 11 (2024), 2547-2555

ASIAN JOURNAL OF CHEMISTRY

https://doi.org/10.14233/ajchem.2024.32333

Adsorption of *ortho*-Nitrophenol from Aqueous Solution using Phosphated Biomass of *Ailanthus excelsa*: Kinetic and Equilibrium Studies

RESHMA S. PAWAR[1], KISAN M. GADAVE[1,2], SHANTANU S. THAKARE[3] and ANANDRAO A. KALE[1,3,*]

[1]P.G. Department of Chemistry and Research Centre and Prof. Ramkrishna More College, Akurdi-411044, India
[2]P.G. Department of Chemistry and Research Centre and, Annasaheb Magar Mahavidyalaya, Hadapsar-411028, India
[3]P.G. Department of Chemistry and Research Centre and, Annasaheb Awate Arts, Commerce & Hutatma Babu Genu Science College, Manchar-410503, India

*Corresponding author: E-mail: anandraoakale@gmail.com

Received: 18 July 2024; *Accepted*: 10 October 2024; *Published online*: 30 October 2024; AJC-21788

This study interprets phosphated biomass of *Ailanthus excelsa* (PBAE) as a eco-friendly, inexpensive and potential adsorbent for adsorption of *ortho*-nitrophenol (ONP) from aqueous solution by using batch adsorption method. The prepared biosorbent was characterized using a variety of techniques such as Brunauer Emmett Teller (BET), Fourier transform infrared spectroscopy (FTIR), X-ray diffraction (XRD) and scanning electron microscope (SEM). As a function of many process parameters including material dose, contact time, concentration, pH and temperature, batch studies were conducted. It was found that a pH of 6.0, a biosorbent dosage of 0.050 g and an initial phenol concentration of 25 mg/L and temperature 298 K were the best conditions for ONP removal. The maximum sorption was found to be 95.28%. Adsorption data was better fitted to the Langmuir, Freundlich, Temkin and Dubinin Radushkevich isotherms. It was demonstrated that the sorption rate follows the pseudo-second order kinetics and intraparticle diffusion theory and the biosorption process was spontaneous and exothermic in nature.

Keywords: Biosorption, Phosphated biomass, *Ailanthus excelsa*, *ortho*-Nitrophenol, Adsorption isotherms.

INTRODUCTION

Different types of pollutants in industrial discharges give rise to environmental risks. To overcome this problem various efforts are continuously carried out for reduction of pollutant concentrations to acceptable standards for the environment [1]. Most common water pollutants includes nitrophenols particularly, *para*-nitrophenol (PNP), *ortho*-nitrophenol (ONP) and chlorophenols are found to be highly toxic to human health and carcinogenic even if present at low concentration [2]. In different research fields and various industries uses such phenolic compounds in wide range and releases these pollutants in surface water [3-5]. Consequently, the United States Environmental Protection Agency (USEPA) recommended the development of effective techniques for the removal of nitro-phenols from wastewater to concentrations below 10 mg/L [6,7]. Several industrial methods are used such as membrane filtration [8], chemical coagulation, occulation [9], photocatalytic degradation [10] and adsorption [11,12] for removal of nitrophenols.

Adsorption of the toxic substances present in wastewater onto a naturally available adsorbent decreases the inhibitory effect of the substances on the microbial activity. Adsorption is easy, stable and may transform harmful molecules into safe ones [13,14]. Activated carbon is the most extensively used adsorbent for nitrophenol removal from wastewater. However, commercial activated carbon has great adsorption characteristics but is expensive, limiting its utilization. To meet this need, it is necessary to look for different, less expensive adsorbents made from naturally occurring waste. Various synthetic, industrial and natural materials have been tested for the removal of toxic pollutants [15], dyes [16], heavy metals [17] and phenols [18] from wastewater. Many reports have observed on the synthesis of activated carbon from readily available, cheaper and biowaste materials. Activated carbons have been prepared from bagasse [19], coconut husk [20], corncob [21], agricultural waste material [22], apricot shell [23], bamboo [24], oil palm fibre [25] and sunflower seed hull [26].

Numerous investigations have revealed that activated carbon, activated carbon fibres or other adsorbents can readily adsorb and eliminate *ortho*-nitrophenol [27-29], but no studies have been focused on *Ailanthus excelsa*. So *Ailanthus excelsa* stem is a biomass whose use has been little explored in literature [30] and can be used as precursor material for activated carbon production due to three main reasons: composition, availability and waste management. The aim of this study was to evaluate the potential of activated carbon prepared from phosphated biomass from *A. excelsa* bark for the *ortho*-nitrophenol removal from aqueous solution under varying of experimental settings, such as solution initial concentration, adsorbent dosage, contact time, pH and temperature. Kinetics, equilibrium and thermodynamic adsorption studies were also performed under different experimental conditions.

EXPERIMENTAL

The surface area of the sample was determined by applying BET method using N_2 adsorption isotherms at 77 K (NOVA touch 1 LX [s/n: 17016123001]). The chemical groups present in the phosphated biomass of *Ailanthus excelsa* were identified by FT-IR spectroscopy (Shimadzu, Prestige 21, Japan). The morphology of the adsorbent was studied using scanning electron microscope (SEM) through FEI Nova Nanosem 450 model. Finally, the X-ray powder diffractometry (XRD) (Siemens D 5000 powder X-ray diffractometer with a Cu$K\alpha$ radiation (λ = 1.5406 Å, 30 kV, 10 mA), using 2θ = 20-80º, was performed to analyze the crystallinity of absorbent.

Preparation of adsorbent: *Ailanthus excelsa* stalks were dried and washed with triple distilled water for removal of any adherent contaminants. The dry biomass was converted into 100 µ particle size using crushing, milling and sieving. This biomass was treated with phosphoric acid and repeatedly rinsed with distilled water to remove all traces of acid and filtered to obtain phosphated carbon. This was dried in oven at 60 ºC for 12 h and then burned in muffle furnace at 500 ºC in nitrogen atmosphere for 1 h. The resulting activated carbon of *A. excelsa* was preserved and used as an adsorbent.

Preparation of adsorbate: *ortho*-Nitrophenol (ONP) used as a adsorbate was of AR grade. All the solutions were prepared with triple distilled water. A stock solution was prepared by dissolving 0.5 g of phenol in 1000 mL of tripled distilled water. The aliquots of ONP were prepared from above stock solution varied between 25 and 100 mg/L by diluting the stock solution up to the required concentration. The solution pH was adjusted to the required value with 0.1 N solution of NaOH and HCl.

Adsorption studies: Adsorption experiments were performed using the batch process. The pH of adsorbate solutions was adjusted in the range of 2, 4, 6, 8 and 10 by using 0.1 N HCl or 0.1 N NaOH solution. Then 25 mL of 25 mg/L adsorbate solution (ONP) at 25 ºC and 0.05 g PBAE were added into 250 mL conical flask and then sample solution was agitated for 30 min at 120 rpm for every pH adsorbate solution.

The study of effect of temperature, experiment was performed using four different 250 mL conical flask. Each flask consisted of 25 mL ONP solution of 25 mg/L, pH at 6.0 and 0.05 g PBAE and then sample solutions were agitated at 120 rpm at 288, 298, 308 and 318 K respectively. The contact time was varied from 5, 10, 15, 30, 60, 90 and 120 min.

To study effect of concentration 0.025 g to 0.100 g of biosorbent and 25 mL of ONP solution with concentrations varying from 25 to 100 mg/L were prepared. Then sample solutions were agitated for 30 min at 120 rpm at 25 ºC for every concentration of ONP solution.

To study effect of contact time 0.025 g to 0.100 g of biosorbent and 25 mL ONP solution with concentrations 25 mg/L was prepared. The contact time was varied from 5, 10, 15, 30, 60, 90 and 120 min at 120 rpm and 25 ºC for every adsorbent dose.

To study effect of adsorbent dose 0.025 g to 0.100 g of biosorbent and 25 mL of ONP solution with 25 mg/L concentrations was prepared. Then the sample solutions were agitated for 30 min at 120 rpm at 25 ºC for every adsorbent dose. The resulting solution was filtered using an Whatman No. 41 filter paper. All the experimental sets were executed in triplicates. The concentration of ONP in solution before and after adsorption was determined using a double beam UV-visible spectrophotometer (Shimadzu, Japan) at 284 nm. It was observed that the filtrate from activated carbon did not reveal any absorbance at this wavelength. The linearity of the calibration curve over the studied concentration range of 25–100 mg/L demonstrates very consistent results.

The amount of ONP adsorbed onto the PBAE, q_e (mg/g), was calculated using the following relationship:

$$q_e = (C_o - C_e)\frac{v}{m} \quad (1)$$

$$\text{Removal } (\%) = \left(\frac{C_o - C_e}{C_o}\right) \times 100 \quad (2)$$

where q_e (mg/g) is the amount of phenolic compound adsorbed at equilibrium after desired contact time of filterate with the biosorbent; C_o (mg/L) and C_e (mg/L) are the initial and equilibrium concentrations, respectively and V (L) is the volume of solution that contains mass m (g) of PBAE biosorbent.

A same experimental process was also carried out for the kinetic studies. At specific time intervals (0-120 min), while the other parameters were fixed, samples were taken from the filtrate to analyze the remaining concentration of ONP. All the adsorption experiments were performed in triplicate and the mean values were taken in the data analysis. The process of kinetic experiments was similar to those of equilibrium tests. The aqueous samples were tested at time intervals 0-120 min and the concentrations of ONP were similarly estimated. The amount of adsorption at time t, q_t (mg/g), was calculated by using eqn. 3:

$$q_t = (C_o - C_t)\frac{V}{W} \quad (3)$$

where C_o and C_t (mg/L) are the liquid-phase concentrations of phenol at initial and at any time t, respectively; V is the volume of ONP solution (L); and W is the dry adsorbent mass used (g).

RESULTS AND DISCUSSION

BET before adsorption of phenol: Multi-point BET (Brunaur-Emmett-Teller) surface area of adsorbent was determined by nitrogen adsorption at 77.35 K. Using the BET method, the precise surface area of PBAE was determined [31]. This study assumes that a cross-sectional area of a nitrogen molecule is 16.2 $Å^2$/mol, whereas PBAE have surface area of 121.292 m^2/g.

FTIR studies: The FTIR spectra before and after adsorption of ONP on PBAE are shown in Fig. 1 and the peaks indicated that PBAE possesses several functional groups at the surface. Fig. 1b shows the peaks at 1139.19, 1540.05 and 2338.00 and 2103.02 cm^{-1} depicted the formation of C-C, C=C, C≡C in the PBAE sample before adsorption. The absorption band at 3400-3300 cm^{-1} is due to a O-H stretching mode of hydroxyl group and adsorbed water. Asymmetry and the shifting of this band at lower wavenumber predict presence of strong hydrogen bonding. Absorption peak at 1149 cm^{-1} is usually found in carbons activated with phosphoric acid, while 1300-1000 cm^{-1} absorption region is characteristic of carbonaceous/phosphorus and phosphor compounds. After the adsorption of ONP on PBAE, the peaks at 3400-3300 cm^{-1} indicates the presence of phenols on biomass PBAE, while the peaks at 1208, 1031 and 1028 cm^{-1} indicate presence of C-C stretching vibrations (Fig. 1a). The peak at 1595 cm^{-1} depicts the presence of aromatic phenolic OH group, whereas a small peak at 1701 cm^{-1} is assigned to C=O stretching vibrations of aldehyde, ketone, carboxylic acids and lactones.

SEM studies: The SEM micrographs of PBAE sorbent before (Fig. 2a-c) and after adsorption (Fig. 2d-f) of ONP at

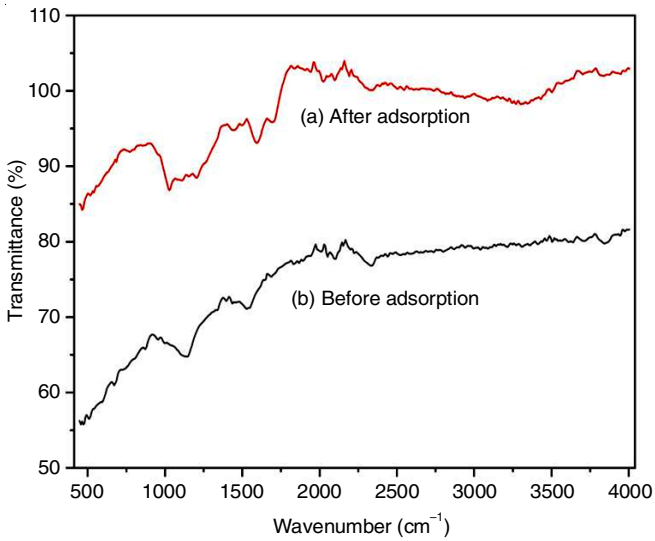

Fig. 1. FTIR spectra of PBAE before and after the adsorption of *o*-nitrophenol

different magnifications are depicted. The external surface of activated carbon formed from PBAE has crevices, cracks and large pores having some grains of various sizes as shown in Fig. 2b and 2c are responsible for adsorption. After adsorption, the higher magnified image taken at 10000X (Fig. 2f) indicated that crystalline structure with irregular shape having particle size ranged from 1.150 µm to 2.205 µm. Figs. 2d and 2e having magnification 1000X and 5000X shows the particles are agglomerized, which might be due to the formation of amorphous nature of biomass after phosphoric acid treatment. Monolayer of the adsorbate molecule over the adsorbent surface is formed

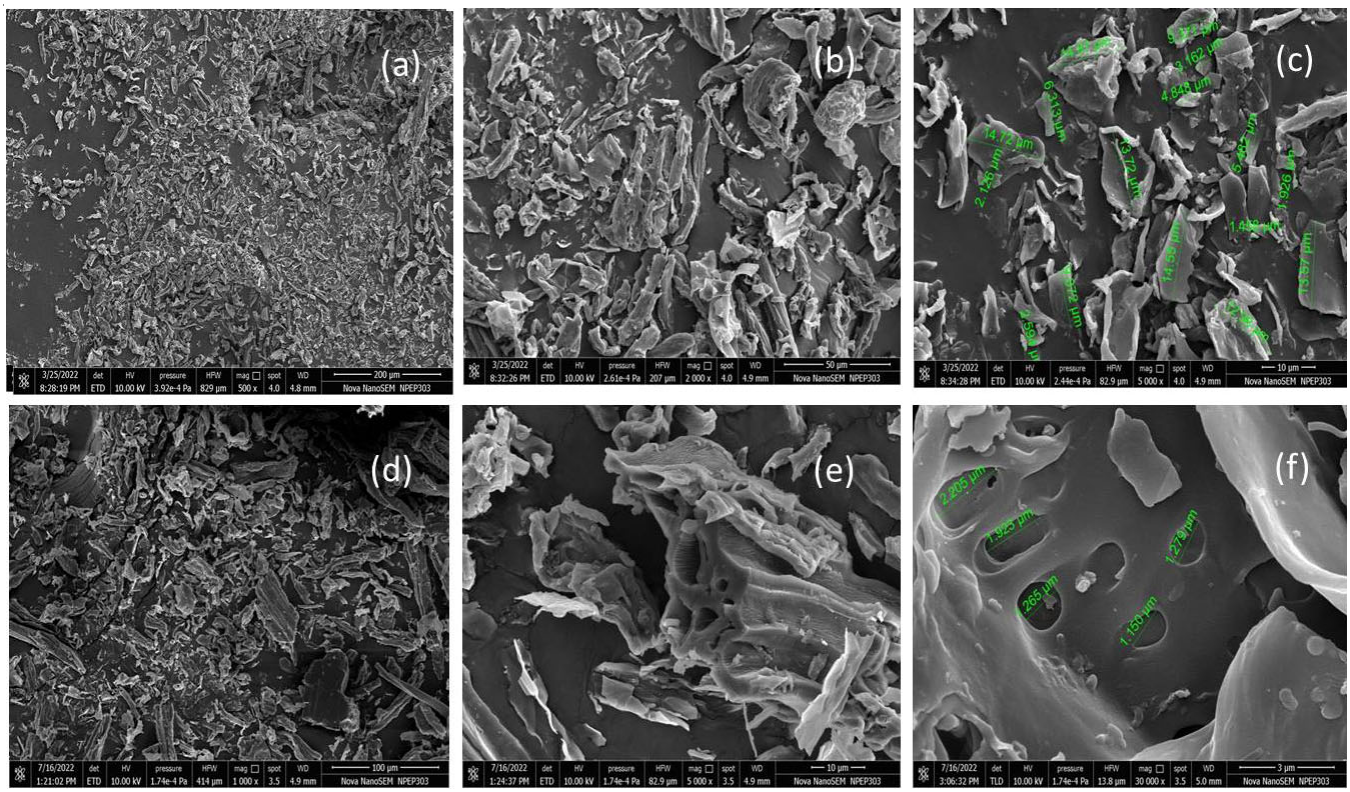

Fig. 2. SEM images of PBAE before and after the adsorption of *o*-nitrophenol

due to covering of the surface of adsorbent because of adsorption. The batch mode adsorption studies conformed well above observations obtained from the SEM studies and also revealed the formation of the molecular cloud of phenol over the surface.

XRD studies: Fig. 3 shows the X-ray diffraction spectra of PBAE (a) after adsorption of ONP (b) before adsorption of ONP. Fig. 3a displays presence of a characteristic main peak of cellulose broad peak at 25.34º was identified as carbon diffraction and an amorphous state of biosorbent. Another typical diffraction corresponding to graphite was detected at 44.28º conforming that PBAE was amorphous carbon with graphite crystal. In comparison of before and after adsorption of ONP, the intensity of above two peaks were significantly increased. The strong and sharp peaks were observed at 22º and 44º, whereas some new peaks also appeared in Fig. 3b at 30.78º, 35.34º, 38.26º and 42.94º which are due to presence of graphite carbon. All these were the evidence of graphitization of PBAE deepening after activation. The average crystallite size of PBAE calculated using Scherrer's equation was found to be 71.26 nm.

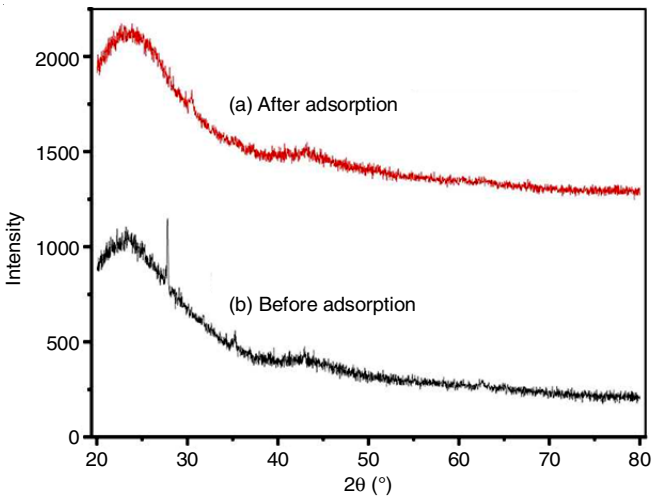

Fig. 3. X-ray diffraction forms of (a) after adsorption of ONP (b) before adsorption of ONP on PBAE

Adsorption studies: Adsorption process variables such as contact time, initial ONP concentration, pH and temperature on absorption rate of ONP were monitored in order to develop the most efficient adsorption kinetic model.

Effect of pH: The adsorption properties are affected by the pH of the solution since carbon surface is amphoteric in nature. Phenol is weak acid and having acid dissociation value (pK_a) of 9.8. At high pH levels, electrostatic repulsion occurs between the negatively charged molecules on the surface of the synthesized carbon and the phenoxide anions in solution, due to the increased concentration of negatively charged phenoxide ions. At lower pH values, the electrostatic attractions increased between the adsorption sites phenolic compounds and phenol. The adsorption reduces progressively up to pH 6, as shown in Fig. 4, but decreases precipitously beyond pH 6. At pHs 2, 4 and 6, there is an significant decrease in the amount of phenol removal showing almost equilibrium. No significant increase in the amount of phenol removed happens with a further rise in pH up to 10. At pH 2, the maximum elimination

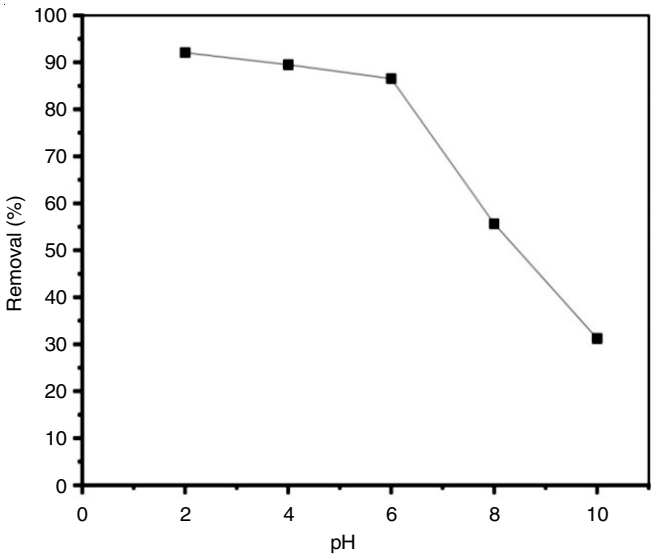

Fig. 4. % Removal *vs*. pH (initial concentration of ONP: 25 mg/L; volume: 25 mL; dosage of PBAE: 0.050 g; contact time: 30 min)

was observed but pH 4 and 6 shows nearby results of ONP % removal. Thus, pH 6.0 is optimized for all the experiments.

Effect of adsorbent dosage: Fig. 5 shows the effect of adsorbent dose on the % removal of ONP. It was observed that the removal percentage of ONP increased with increase in adsorbent dose of PBAE. After the equilibrium time, the removal was 92.28 to 94.24% for adsorbent dosage of 0.025 to 0.100 g. The elimination of ONP increases due to an increase sorption surface area and the availability of additional adsorption sites. It was concluded that at more the carbon to solute concentration ratios, higher sorption takes place on the adsorbent surface; therefore it creates a lower solute concentration in the solution. It was found that the optimum adsorbent dosage was 0.05 g.

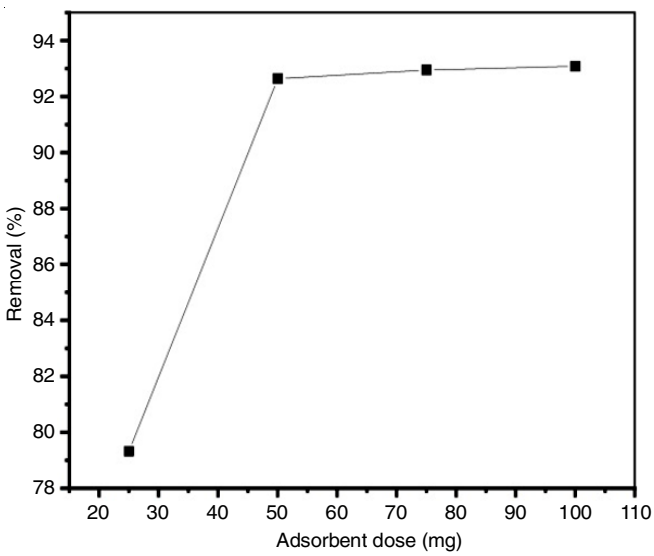

Fig. 5. % Removal *vs*. adsorbent dose (the initial concentration: 25 mg/L; dosage: 0.025 g to 0.100 g; contact time: 30 min; volume: 25 mL; pH: 6; temp. 25 °C)

Effect of contact time: Adsorption efficiency of ONP by PBAE was changed with contact time (Fig. 6). Maximum adsor-

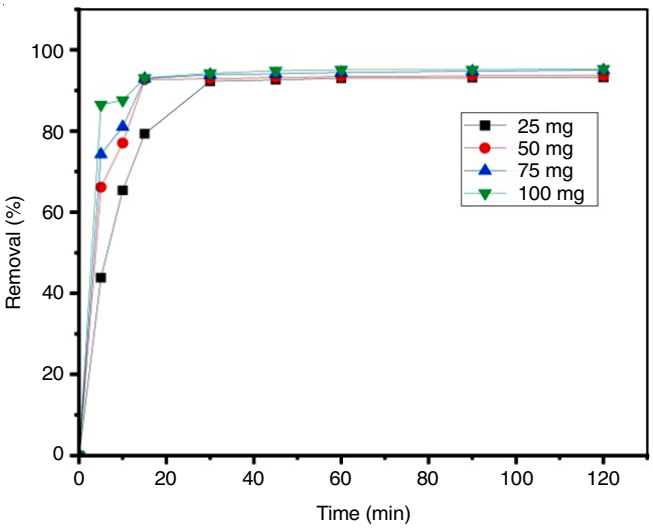

Fig. 6. % Removal *vs*. contact time (initial concentration: 25 mg/L; dosage: 0.025 g to 0.100 g; volume: 25 mL; pH: 6; temp. 25 °C)

ption of ONP taken place within the first 15 min, under separate doses of PBAE. After 15 min, the adsorption capacity gradually increased as contact time extended due to a reduction in driving force after prolonged reaction. However, the adsorption achieved equilibrium in less than 60 min.

Effect of initial concentration: The effect of initial ONP concentration on % removal of ONP is shown in Fig. 7, which was evaluated at 25, 50, 75 and 100 mg/L at pH 6, temperature 25 ºC and contact time of 30 min. The results show that the biosorption capacity decreases with increasing initial ONP concentration. At the initial stage, the adsorption rate is higher, due of accessibility of additional numbers of vacant sites. After a definite time period as concentration increases from 25-100 mg/L, the rate of adsorption decreases because of aggregation of adsorbate in the vacant sites. The initial concentration provides the necessary driving power to regulate all mass transfer resistance of molecules between the solid and aqueous phases.

Effect of temperature: The effect of temperature on the ONP biosorption process was investigated at 298, 308, 318 and 328 K. The capacity to adsorb phenol decreases as temperature rises, which indicates that ONP uptake process was exothermic (Fig. 8). This was due to weakening of bonds between the molecules of nitrophenol and the biosorbents active site. The solubility of ONP rises with an increase in solution temperature, consequently, the contact forces between the solute and solvent are intensified. Therefore, the solute is more challenging to adsorb at higher temperatures.

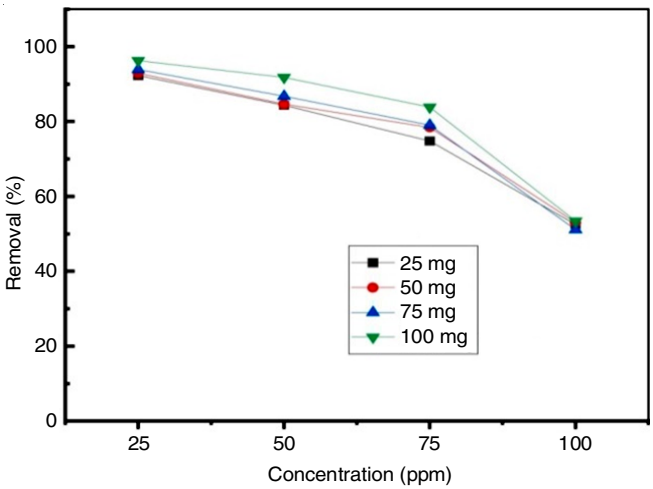

Fig. 7. % Removal *vs*. concentration (ppm) (Initial concentration: 25 to 100 mg/L; dosage: 0.025-0.100g; volume: 25 mL; pH: 6; temp.: 25 °C)

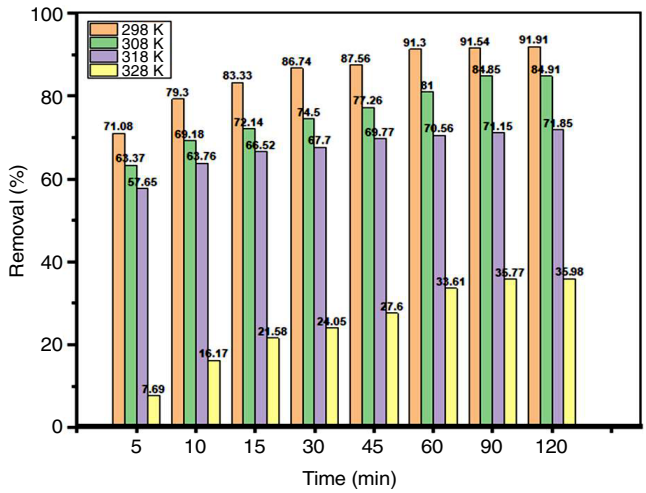

Fig. 8. Effect of temperature on % removal *vs*. contact time (the initial concentration: 25 mg/L; dosage: 100 mg; volume: 25 mL; contact time 0-120 min; pH: 6)

Adsorption isotherms: The adsorption isotherm is essential for comprehending the solute-adsorbent interaction as well as the quantity of adsorbate retained on the adsorbent and the concentration of adsorbate in solution at equilibrium under constant temperature conditions. In this study, the two-parameter isotherms proposed by Temkin, Langmuir and Freundlich and three-parameter isotherm proposed by Dubinin-Radushkevich (D-R) isotherms were examined.

The Langmuir isotherm demonstrated that the adsorption process occurs only on the adsorbent surface with a uniform distribution of energy levels [32]. Once the adsorbate is adhered on the site, no more adsorption takes place which indicates that adsorption is monolayer. The equation of Langmuir isotherm is:

$$\frac{1}{q_e} = \frac{1}{q_m} + \frac{1}{K_L q_m C_e} \quad (4)$$

where K_L is Langmuir constant (L/mg) associated to the affinity of binding sites as well as with the free energy of sorption; q_e is ONP concentration at equilibrium onto biosorbent (mg/g); C_e is ONP concentration at equilibrium in solution (mg/L); and q_m is the ONP concentration when monolayer formed on the PBAE (biosorbent). The separation factor "R_L" shows the nature of the adsorption process [33]. The R^2 value obtained from Langmuir model was 0.8251 as shown in Fig. 9a, which is low as compared to Temkin and D-R isotherms.

Freundlich isotherm [34,35] shown in Fig. 9b demonstrates that the adsorption arises on the heterogeneous sites with the irregular separation of energy level and also implies the

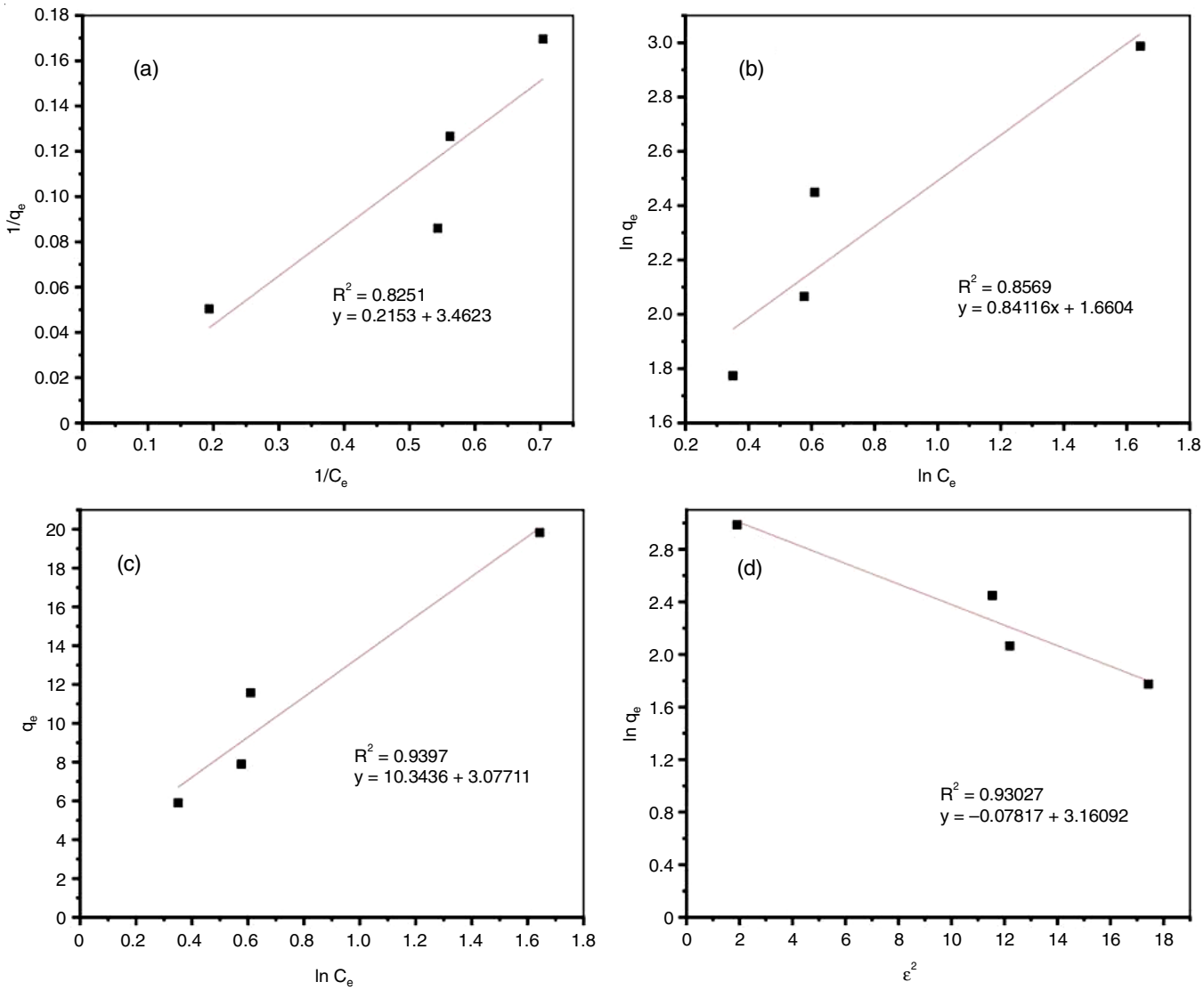

Fig. 9. Isotherm models (a) Langmuir Isotherm (b) Freundlich isotherm (c) Intraparticle diffusion (d) Dubinin-Radushkevich isotherm

reversible adsorption and multilayer adsorption. The mathematical equation of heterogeneous surface system is represented as:

$$\ln q_e = \ln K_F + \frac{1}{n}\ln C_e \quad (5)$$

where q_e is the amount of adsorbate adsorbed at equilibrium (mg/g); C_e is equilibrium concentration of the adsorbate (mg/L); K_F is the Freundlich constant (mg/g) and 1/n is adsorption intensity. The value of n > 1 indicates favourable adsorption condition.

The Temkin isotherm [36], illustrated in Fig. 9c, demonstrates the predominance of indirect adsorbate/adsorbate interactions within adsorption isotherms, indicating that the heat of adsorption for all molecules in the layer diminishes linearly with increasing involvement due to these interactions. The following equation provides the linearized Tempkin equation:

$$q_e = \beta \ln \alpha + \beta \ln C_e \quad (6)$$

where T is the absolute temperature in Kelvin; R is the universal gas constant (8.314 J/mol K); b is the Tempkin constant related to heat of sorption (J/mg). The slope and intercept of q_e *vs.* ln C_e are used to determine the Temkin constants a and b.

To evaluate the specific porosity of the biomass and probable energy of adsorption, the Dubinin-Radushkevich model [37, 38] was used. The mathematical equation for adsorption isotherm given by Dubinin-Radushkevich is:

$$\ln q_e = \ln q_m - \beta \varepsilon^2 \quad (7)$$

where β (mmol^2 J^{-2}) is D-R constant; ε (J mmol^{-1}) is Polanyi potential

$$\varepsilon = RT \ln\left(1 + \frac{1}{C_e}\right) \quad (8)$$

where R (8.314 J mol^{-1} K^{-1}) is the universal gas constant; T is the temperature (K). Here β is related to the free energy of adsorption per mole of adsorbate as it migrates to the surface of biomass from infinite distance in solution. Fig. 9d shows plot of ln q_e *vs.* ε^2 for ONP concentration 25 mg/L. The graph gives values of q_m and β from slope and intercepts values. Porosity parameter value β for activated PBAE towards phenol was less than unity indicating sorption of phenol was significant.

TABLE-1
RESULTS OF ISOTHERM PLOTS FOR THE ADSORPTION OF ONP ONTO PBAE

Models	Isotherm constants		
Langmuir	q_m (mg/g) = 4.6446	K_L (L/mg) = 0.06218	R^2 = 0.8251
Freundlich	n = 1.1888	K_F (mg/g) = 4.4668×10^{-1}	R^2 = 0.8591
Tempkin	I (l/g) = 805.1619	K_T (L/mg) = 0.09667	R^2 = 0.9306
Dubinin-Radushkevich	Qm = -12.7926	$\beta = 0.7817 \times 10^{-1}$	R^2 = 0.93027

The experimental data and calculated isotherm constants are shown in Table-1. The expected theoretical isotherms for the adsorption of PBAE are shown in Fig. 9 indicates that Temkin isotherm model is the best fit model when compared to other studied isotherm models for adsorbent treated with phosphoric acid. This indicates that PBAE has strong adsorbate relation with adsorption isotherm.

Thermodynamic studies: For the ONP adsorption onto PBAE, the free energy change (ΔGº), enthalpy change (ΔHº) and entropy change (ΔSº) have been examined as thermodynamic parameters to estimate the feasibility of the adsorption process. Eqn. 9 was used to calculate these parameters:

$$\Delta G^\circ = -2.303\ RT \log K_d \quad (9)$$

where R is the universal gas constant (8.314 J/mol K). The values of ΔHº and ΔSº were determined by the slope and intercept of the ln K_d against 1/T (Fig. 10). Using eqn. 9, the Gibb's free energy change of sorption ΔGº was determined. Due to the expansion of pore size and activation of the sorbent surface with temperature, PBAE's adsorption capacity increased. The findings indicated that ONP adsorption is an exothermic process. The thermodynamic parameters for ONP adsorption are shown in Table-2. The exothermic nature of the reaction involving the adsorption of ONP onto PBAE is indicated by the negative value of ΔHº (-0.9154 kJ/mol^{-1}). The computed value of ΔGº (456.66 KJ mol^{-1}) indicates the spontaneous adsorption process. Additionally, the positive entropy change value, ΔSº (252.888), illustrates the PBAE's affinity for ONP.

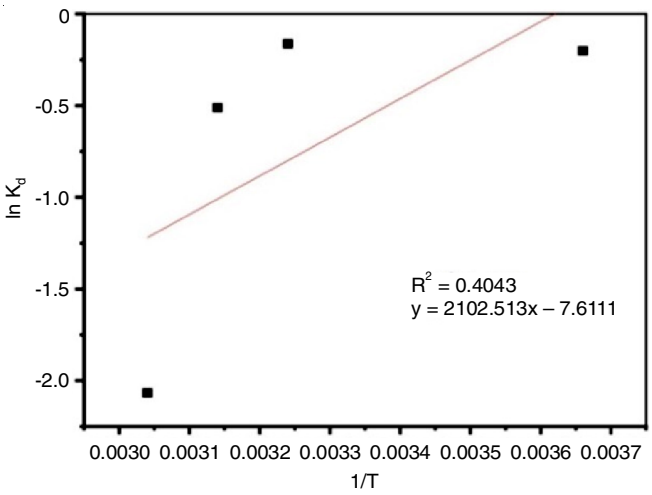

Fig. 10. ln K_d *vs.* 1/temperature

Adsorption kinetics studies: The pseudo-first-order and pseudo-second-order and Elovich models were applied to examine the adsorption of ONP on PBAE while intraparticle diffusion model was applied to examine the adsorption mechanism [39]. The slope as well as intercept of the linear plots of t/q_t *versus* time (min) was used to derive the kinetic parameters. Based on R^2 values (linear regression correlation coefficient) the best-fit model was chosen. The plots of log ($q_e - q_t$) *vs.* time (Fig. 11a), t/q_t *vs.* time (Fig. 11b) and q_t *vs.* ln t (Fig. 11c) shows the first order, second order and Elovich kinetic plots, respectively. A linear relationship indicates applicability of first and second order kinetics. The linear plots of t/q_t *versus* time (Fig. 11b) show a good agreement between experimental and calculated q_e values. The correlation coefficients (R^2) for the second-order kinetic model was 0.9980 > Elovich model was 0.81413 > first order kinetic model was 0.32442 indicating the highest applicability of this kinetic equation and the second-order nature of the adsorption of ONP by PBAE. The results shows that as the quantity of adsorbent dosage increased, the values of K_2 were also increased while q_e appreciably reduced (Table-2).

The kinetics results were also analyzed by intraparticle diffusion model to interpret the diffusion mechanism. The expression for the intraparticle diffusion equation is represented as:

$$q_t = K_d\, t^{1/2} + C \quad (10)$$

where K_d (mg/g min 1/2) stands for the intraparticle diffusion rate constant. It is evident from the graphical representation Fig. 11a that the linear part of the plot does not cross the origin. The variation in the mass transfer between both initial and final stages of the origin suggests that the ONP adsorption on the PBAE, the adsorption process could be the reason of this process from prepared *A. excelsa* plant involved several steps, including adsorption on the exterior surface and diffusion into the interior.

Fig. 12b plot of q_t *vs.* $t^{0.5}$ shows more than one linear portions indicating that adsorption was due to more than one

TABLE-2
KINETIC (PSEUDO FIRST ORDER AND PSEUDO SECOND ORDER AND ELOVICH MODEL) AND THERMODYNAMIC PARAMETERS FOR THE SORPTION OF ONP ONTO PBAE

Pseudo first order model	k_1 (min^{-1}) = 0.00318	q_e (mg/g) = 106.0425	R^2 = 0.3244
Pseudo second order model	k_2 (g/(mg min) = 12.82×10^{-3}	q_e = 24.01	R^2 = 0.9980
Intraparticle diffusion model	K_d (mg/g min) = 5.0245	C (mg/g) = 2.8976	R^2 = 0.9367
Elovich	B = 7.8268	A(m) slope = 3.6966	R^2 = 0.81413
Thermodynamic parameter	ΔH° (kJ/mol) = -0.9154	ΔS° (J/mol K) = 252.888	ΔG° (kJ/mol) = 456.66

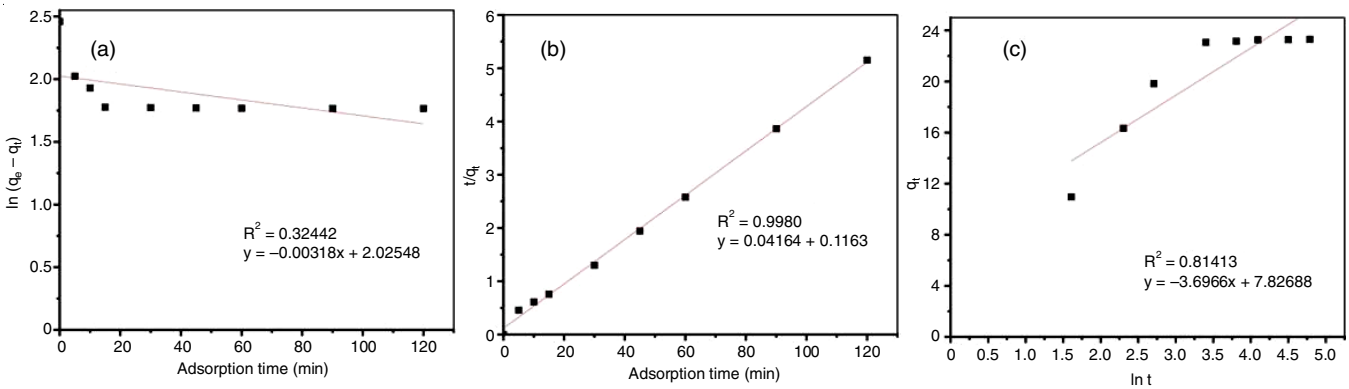

Fig. 11. Pseudo first order (a), pseudo second order (b) and Elovich (c) kinetic plot

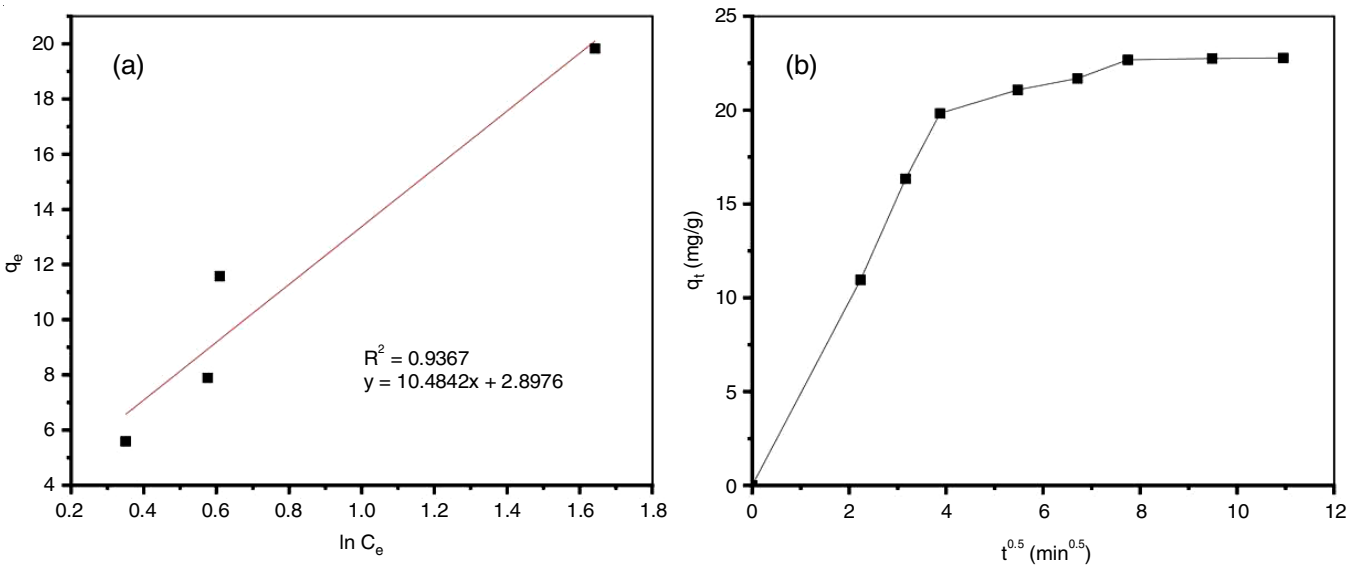

Fig. 12. Intraparticle diffusion plot for adsorption of *ortho*-nitrophenol onto PBAE at 25 ºC for 25 ppm

process. It shows adsorption process involves two steps. The external surface adsorption stage is shown by the sharp increasing part, whereas the gradual adsorption step, which involves pore diffusion or intraparticle, is shown by the second gradually increasing linear part. The deviation from origin for the slow adsorption phase indicated in Fig. 12a indicates that intraparticle diffusion is not only the rate limiting step and external surface adsorption step happens, which might be used to explain mechanism of adsorption process.

Conclusion

The phosphated biomass of *Ailanthus excelsa* (PBAE) was subjected to extensive characterizations using different techniques such as BET, FTIR, SEM and XRD. Batch experiments were performed as functions of different variables such as pH, temperature, initial phenol concentration and biosorbent dose. The maximum sorption for this adsorbate was occurred at concentration 25 mg L^{-1}/25 mL, sorbent dosage 0.050 g/25 mL, contact time 15 min and temperature 288 K were observed. The equilibrium data were fitting in the Langmuir, Freundlich, Temkin and Dubinin-Radushkevich isotherm models which approved that the sorption is heterogeneous and occured through the physico-chemical interactions. The rate of sorption was found to obey pseudo-second order kinetics and intraparticle diffusion model with correlation coefficient value is 0.9980 and 0.9367. The negative ΔG^{o} values indicated that the sorption of *ortho*-nitrophenol (ONP) onto biosorbent was spontaneous, whereas the negative ΔH^{o} value illustrated the exothermic nature of the sorption.

ACKNOWLEDGEMENTS

The authors are thankful to the Principal & Head, Department of Chemistry, Annasaheb Awate College, Manchar, India for providing the infrastructural facilities and seed money to complete this research work. Thanks are also due Central Instrumentation Facility, Savitribai Phule Pune University, Pune, India for providing the instrumental facilities.

CONFLICT OF INTEREST

The authors declare that there is no conflict of interests regarding the publication of this article.

REFERENCES

1. A.A. Oyekanmi, A.A.A. Latiff, Z. Daud, R.M.S.R. Mohamed, N.A.A. Aziz, N. Ismail, M. Rafatullah, A. Ahmad and K. Hossain, *Desalination Water Treat.*, **169**, 181 (2019); https://doi.org/10.5004/dwt.2019.24689

2. M. Aazza, C. Mounir, H. Ahlafi, A. Bouymajane and F. Cacciola, *J. Mol. Liq.*, **383**, 122139 (2023); https://doi.org/10.1016/j.molliq.2023.122139
3. M. Ahmaruzzaman, S.R. Mishra, V. Gadore, G. Yadav, B. Bhattacharjee, S. Roy, A. Bhuyan, B. Hazarika, J. Darabdhara and K. Kumari, *J. Environ. Chem. Eng*., **12**, 112964 (2024); https://doi.org/10.1016/j.jece.2024.112964
4. M.C. Tomei, M.C. Annesini, S. Rita and A.J. Daugulis, *Environ. Sci. Technol.*, **44**, 7254 (2010); https://doi.org/10.1021/es903806p
5. S. Yi, W.Q. Zhuang, B. Wu, S.T.L. Tay and J.H. Tay, *Environ. Sci. Technol.*, **40**, 2396 (2006); https://doi.org/10.1021/es0517771
6. WHO/UNICEF Joint Water Supply, Sanitation Monitoring Programme Progress on Drinking Water and Sanitation, Update (2014).
7. T. Deblonde, C. Cossu-Leguille and P. Hartemann, *Int. J. Hyg. Environ. Health*, **214**, 442 (2011); https://doi.org/10.1016/j.ijheh.2011.08.002
8. D.P. Zagklis, A.I. Vavouraki, M.E. Kornaros and C.A. Paraskeva, *J. Hazard. Mater.*, **285**, 69 (2015); https://doi.org/10.1016/j.jhazmat.2014.11.038
9. H.J. Choi, *Biotechnol. Biotechnol. Equip.*, **29**, 666 (2015); https://doi.org/10.1080/13102818.2015.1031177
10. A. Turki, C. Guillard, F. Dappozze, Z. Ksibi, G. Berhault and H. Kochkar, *Appl. Catal. B*, **163**, 404 (2015); https://doi.org/10.1016/j.apcatb.2014.08.010
11. A. Bhatnagar, W. Hogland, M. Marques and M. Sillanpää, *Chem. Eng. J.*, **219**, 499 (2013); https://doi.org/10.1016/j.cej.2012.12.038
12. P.S. Thue, M.A. Adebayo, E.C. Lima, J.M. Sieliechi, F.M. Machado, G.L. Dotto, J.C.P. Vaghetti and S.L.P. Dias, *J. Mol. Liq.*, **223**, 1067 (2016); https://doi.org/10.1016/j.molliq.2016.09.032
13. W.J. Weber Jr. and J.C. Morris, *J. Sanit. Engrg. Div.*, **89**, 31 (1963); https://doi.org/10.1061/JSEDAI.0000430
14. M.A. Abdelaziz, M.M. Abdelaziz, H.M. Althurwi, I.A. Algrfan, K.M. Alasiri and S.K. Mustafa, *Asian J. Chem. Sci.*, **14**, 65 (2024); https://doi.org/10.9734/ajocs/2024/v14i1287
15. A.F. Alkaim, A.M. Aljeboreea, O.H. Salahb, A.A. Aljanabic and U.S. Altimarid, *Asian J. Green Chem.*, **8**, 188 (2024); https://doi.org/10.48309/ajgc.2024.427437.1467
16. R. Al-Tohamy, S.S. Ali, F. Li, K.M. Okasha, Y.A.-G. Mahmoud, H. Jiao, T. Elsamahy, Y. Fu and J. Sun, *Ecotoxicol. Environ. Safety*, **231**, 113160 (2022); https://doi.org/10.1016/j.ecoenv.2021.113160
17. C. Femina-Carolin, T. Kamalesh, P. Senthil Kumar, G. Rangasamy, *Ind. Chem. Chem. Res*., **62**, 8575 (2023); https://pubs.acs.org/doi/10.1021/acs.iecr.3c00709
18. R.S. Juang, F.C. Wu and R.L. Tseng, *Colloids Surf. A Physicochem. Eng. Asp.*, **201**, 191 (2002); https://doi.org/10.1016/S0927-7757(01)01004-4
19. R.R. Karri, N.S. Jayakumar and J.N. Sahu, *J. Mol. Liq.*, **231**, 249 (2017); https://doi.org/10.1016/j.molliq.2017.02.003
20. I.A.W. Tan, A.L. Ahmad and B.H. Hameed, *J. Hazard. Mater.*, **154**, 337 (2008); https://doi.org/10.1016/j.jhazmat.2007.10.031
21. R.L. Tseng and S.K. Tseng, *J. Colloid Interface Sci.*, **287**, 428 (2005); https://doi.org/10.1016/j.jcis.2005.02.033
22. K.P. Singh, A. Malik, S. Sinha and P. Ojha, *J. Hazard. Mater.*, **150**, 626 (2008); https://doi.org/10.1016/j.jhazmat.2007.05.017
23. B. Karagozoglu, M. Tasdemir, E. Demirbas and M. Kobya, *J. Hazard. Mater.*, **147**, 297 (2007); https://doi.org/10.1016/j.jhazmat.2007.01.003
24. B.H. Hameed, A.T.M. Din and A.L. Ahmad, *J. Hazard. Mater.*, **141**, 819 (2007); https://doi.org/10.1016/j.jhazmat.2006.07.049
25. I.A.W. Tan, B.H. Hameed and A.L. Ahmad, *Chem. Eng. J.*, **127**, 111 (2007); https://doi.org/10.1016/j.cej.2006.09.010
26. N. Thinakaran, P. Baskaralingam, M. Pulikesi, P. Panneerselvam and S. Sivanesan, *J. Hazard. Mater.*, **151**, 316 (2008); https://doi.org/10.1016/j.jhazmat.2007.05.076
27. A.J.K. Kupeta, E.B. Naidoo and A.E. Ofomaja, *J. Clean. Prod.*, **179**, 191 (2018); https://doi.org/10.1016/j.jclepro.2018.01.034
28. E.R. Abaide, G.L. Dotto, M.V. Tres, G.L. Zabot and M.A. Mazutti, *Bioresour. Technol.*, **284**, 25 (2019); https://doi.org/10.1016/j.biortech.2019.03.110
29. T. Sismanoglu and S. Pura, *Colloids Surf. A Physicochem. Eng. Asp.*, **180**, 1 (2001); https://doi.org/10.1016/S0927-7757(00)00751-2
30. A. Kale and R. Pawar, *J. Emerg. Technol. Innov. Res.*, **8**, c446 (2021).
31. V.C. Srivastava, M.M. Swamy, I.D. Mall, B. Prasad and I.M. Mishra, *Colloids Surf. A Physicochem. Eng. Asp.*, **272**, 89 (2006); https://doi.org/10.1016/j.colsurfa.2005.07.016
32. I. Langmuir, *J. Am. Chem. Soc.*, **38**, 2221 (1916); https://doi.org/10.1021/ja02268a002
33. V. Srihari and A. Das, *Desalination*, **225**, 220 (2008); https://doi.org/10.1016/j.desal.2007.07.008
34. H.M.F. Freundlich, *Z. Phys.Chem.*, **57**, 385(1906).
35. Y.S. Ho and G. McKay, *Chem. Eng. J.*, **70**, 115 (1998); https://doi.org/10.1016/S0923-0467(98)00076-1
36. S. Veli and B. Alyüz, *J. Hazard. Mater.*, **149**, 226 (2007); https://doi.org/10.1016/j.jhazmat.2007.04.109
37. Y. Huang, X. Ma, G. Liang and H. Yan, *Chem. Eng. J.*, **141**, 1 (2008); https://doi.org/10.1016/j.cej.2007.10.009
38. S. Chowdhury and P.D. Saha, *Colloids Surf. B Biointerfaces*, **88**, 697 (2011); https://doi.org/10.1016/j.colsurfb.2011.08.003
39. Y.S. Ho and G. McKay, *Water Res.*, **34**, 735 (2000); https://doi.org/10.1016/S0043-1354(99)00232-8